

Chiral Nematic Phase of Suspensions of Rodlike Viruses: Left-Handed Phase Helicity from a Right-Handed Molecular Helix

Fabio Tombolato,¹ Alberta Ferrarini,¹ and Eric Grelet²

¹*Dipartimento di Scienze Chimiche, Università di Padova, via Marzolo 1, 35131 Padova, Italy*

²*Centre de Recherche Paul Pascal, CNRS UPR 8641, Université Bordeaux I, 115 Avenue Albert Schweitzer, 33600 Pessac, France*

(Received 13 April 2006; published 28 June 2006)

We report a study on charged, filamentous virus called M13, whose suspensions in water exhibit a chiral nematic (cholesteric) phase. In spite of the *right*-handed helicity of the virus, a *left*-handed phase helicity is found, with a cholesteric pitch which increases with temperature and ionic strength. Several sources of chirality can be devised in the system, ranging from the subnanometer to the micrometer length scale. Here an explanation is proposed for the microscopic origin of the cholesteric organization, which arises from the helical arrangement of coat proteins on the virus surface. The phase organization is explained as the result of the competition between contributions of opposite handedness, deriving from best packing of viral particles and electrostatic interparticle repulsions. This hypothesis is supported by calculations based on a coarse-grained representation of the virus.

DOI: [10.1103/PhysRevLett.96.258302](https://doi.org/10.1103/PhysRevLett.96.258302)

PACS numbers: 82.70.-y, 61.30.-v, 61.30.Cz, 61.30.St

Filamentous viruses are long and thin polyelectrolytes, made of a filament of nucleic acid, enclosed in a cylindrical wrapping of proteins (capsid). Features like monodispersity, some degree of stiffness, and the ability to organize in ordered structures motivate the strong interest they have raised as model systems for soft condensed matter physics [1]. Filamentous viruses form liquid crystalline phases [2], whose general behavior, i.e., transition properties and degree of order, can be explained in terms of a few parameters, as density, contour length (L), diameter (D), and surface charge density, according to theories developed for colloidal dispersions of rodlike polyelectrolytes that experience steric and screened electrostatic interactions [3,4]. Ion mediated electrostatic interactions between virions can also explain the bundling behavior of M13 and *fd* viruses [5]. However, the connection between chirality at the molecular scale and the macroscopic chiral organization of liquid crystalline phases is not understood, and the prediction of twist handedness and periodicity (cholesteric pitch) based on molecular features remains a challenge [6,7]. A puzzling example is provided by Pf1 and *fd* bacteriophages, which have similar structures and slightly different arrangements of proteins on the surface [8,9]: *fd* exhibits a cholesteric phase, whereas only a nematic phase has been found for Pf1 [10]. Another surprising result is the persistence of phase chirality when filamentous viruses are sterically stabilized with a thick coat of neutral polymer [7]. If, in general, the connection between molecular and phase chirality is not straightforward [6], the complexity becomes even higher in the case of viruses, due to the simultaneous presence of several levels of chirality. These range from the asymmetry of C_α atoms in the coat proteins, to the α -helical structure of these proteins and their helical arrangement on the virus surface. The observation of phase chirality for polymer stabilized viruses led to the sugges-

tion of an influence of chiral fluctuations of the virus shape [7].

In this Letter, we shall focus on the cholesteric phase formed by M13 virus [8]. In addition to the dependence of the cholesteric pitch on temperature and ionic strength, we have measured the handedness, which is essential to fully characterize a chiral system, but is sometimes neglected. An explanation for the origin of the phase chirality is proposed and tested with the help of a molecular model.

M13 is a charged monodisperse bacteriophage with a high aspect ratio ($L = 880$ nm, $D = 6.6$ nm); M13 is semiflexible (persistence length $\xi = 2200$ nm) and has a molecular weight of $M_w = 1.64 \times 10^7$ g/mol [10]. M13 is formed by a single stranded DNA, around which about 2700 identical coat proteins are helicoidally wrapped following a fivefold rotation axis combined with a twofold screw axis [8,11]. The model of the M13 virus surface is shown in Fig. 1. A coat protein is formed by 50 amino acids, which provide M13 with a helical charge distribution; a net charge (carried by ionic amino acids) of $-2.4e$ per protein in water at $pH = 8.2$ is estimated, i.e., a linear charge density of about $7e/\text{nm}$ [8,12]. Taking advantage of the colloidal scale, which allows the visualization by fluorescence microscopy of a *single* rodlike virus, the cholesteric handedness of aqueous suspensions of M13 rods has been determined [13]. Relatively thick glass cells made by cover slip and slide have been used, with mylar spacers of different thicknesses (50 and 100 μm) to avoid boundary effects. Samples are equilibrated for 24 hours, which leads to planar cholesteric domains (cholesteric helix axis parallel to the incident light) with a size of a few hundred μm (Fig. 2). *Left*-handed supramolecular helicity is observed, whereas *right* handedness would be expected for purely steric reasons. Indeed, a simple steric model, extended from Straley's work for the packing of helical structures

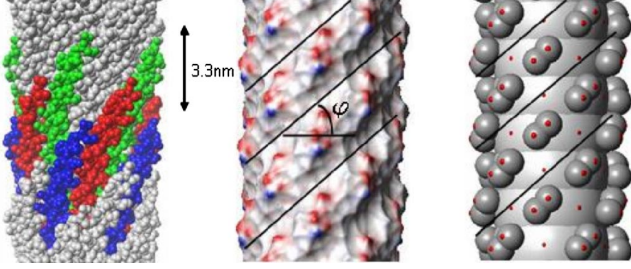


FIG. 1 (color online). Surface of the M13 virus [24], generated from the 2C0X.pdb capsid protein structure [8]. (a) All-atom representation; proteins with a given color are related by a fivefold symmetry axis. The distance of 3.3 nm corresponds to the periodicity, i.e., the separation between pairs of proteins with the same coordinates in the plane perpendicular to this symmetry axis. (b) Surface accessible to a sphere of radius 0.5 nm, rolling on the all-atom representation. Colors correspond to the electrostatic potential (red: negative, blue: positive). (c) Coarse-grained representation. Stacked light gray spheres (radius of 2.5 nm) represent the core of the virus, while dark gray spheres (radius of 0.6 nm) represent protruding amino acids (each sphere corresponds to 4 amino acids). Red spots correspond to point charges (located at 0.1 nm distance from the virus surface). Black lines show the tangent to a right-handed molecular helix identified on the virus surface ($\varphi \sim 41^\circ$).

[14], shows that right-handed screws pack in a right-handed way for $\varphi < 45^\circ$, whereas a left-handed superhelix is generated for $\varphi > 45^\circ$ [Fig. 1(b)] [6]. The cholesteric pitch p , or correspondingly the wave number $q = 2\pi/p$, is defined as positive or negative, according to the right or left handedness of the cholesteric helix, respectively. Its ex-

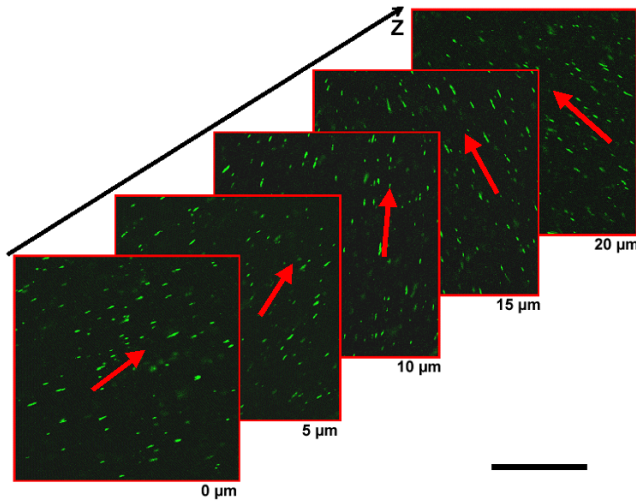


FIG. 2 (color online). Direct visualization by confocal fluorescence microscopy of the left-handed cholesteric helix in M13 virus suspensions, at concentration $C_{M13} = 49$ mg/ml and ionic strength $I = 110$ mM. The sequence of images follows the virus director, represented by red arrows, through the sample thickness (Z). One M13 virus out of 10^4 has been labeled with a fluorescein dye. The scale bar indicates $50 \mu\text{m}$.

perimental dependence upon temperature and ionic strength has also been measured (Table I), using polarization microscopy [7,10].

The cholesteric phase of M13 shares some similarity with that of right-handed B-DNA, where a left-handed helicity has been found by circular dichroism [15]. Recently, a model for the latter has been proposed, interpreting the cholesteric organization as the result of the competition of steric and electrostatic repulsion between charged helices [16]. The main responsibility for the chiral supramolecular organization has been ascribed to the shape chirality, which would also modulate the electrostatic repulsion between DNA molecules. We have hypothesized a similar mechanism for M13. Although not so clearly defined as in the case of DNA, a right-handed helix can be identified on the surface structure of M13 (Fig. 1). As a consequence of the geometrical arrangement of the major coat proteins and the mobility of their solvent exposed N -terminal portion [8,11], grooves as deep as about 1 nm appear on the virus surface. Their presence and dimension is supported by x-ray data, showing that pentapeptides can be inserted between two adjacent α helices on the surface of the virion [17]. Since each protein bears some ionic charges, the chiral arrangement of the coat implies a helical charge distribution (Fig. 1). The possibility that shape and charge chirality deriving from the protein arrangement can be responsible for the cholesteric organization has been explored with a theoretical approach. According to the continuum elastic theory, the Frank free energy density f can be expanded in a power series of the twist deformation of the mesophase director: $f \approx f^u + K_t q + \frac{1}{2} K_{22} q^2$, where f^u is the free energy density of the undeformed nematic phase [18]. The equilibrium wave number is obtained by minimization of the free energy: $q = -K_t/K_{22}$, with the chiral strength $K_t = (\partial f / \partial q)_{q=0}$ and the twist elastic constant $K_{22} = (\partial^2 f / \partial q^2)_{q=0}$. K_t accounts for the intrinsic propensity to twist deformations, as a consequence of the chirality of intermolecular interactions; it has opposite signs for enantiomers, and vanishes in the absence of molecular chirality. K_{22} describes the resistance of the system to the director deformation. A molecular expression for the free energy has been developed with a pair potential consisting of steric repulsions and electrostatic interactions between virus particles in an ionic water solution [16]. The former are treated at the level of the second virial term, while the latter have been included by averaging over the hard-particle pair distribution function, according to the mean field approximation. The excess Helmholtz free energy of a suspension of N virus particles can then be expressed as:

$$F^{\text{ex}} = \frac{1}{2} \int d\mathbf{R}_A d\mathbf{R}_B d\Omega_A d\Omega_B \rho(\Omega_A, \mathbf{R}_A) \times \rho(\Omega_B, \mathbf{R}_B) u(\mathbf{R}_{AB}, \Omega_{AB}), \quad (1)$$

where \mathbf{R} and Ω denote position and orientation of a virion

TABLE I. Order parameter (\overline{P}_2), twist elastic constant (K_{22}), steric (K_t^h), and electrostatic (K_t^{el}) contributions to the chiral strength, and cholesteric wave number: q^{calc} (calculated), q_h^{calc} (calculated for purely hard-core interactions), and q^{exp} (experimental). T is temperature and I the ionic strength. The virus concentration is $C_{\text{M13}} = 53$ mg/ml.

T (K)	I (mM)	\overline{P}_2	K_{22} (pN)	K_t^h (nN/m)	K_t^{el} (nN/m)	q^{exp} (μm^{-1})	q^{calc} (μm^{-1})	q_h^{calc} (μm^{-1})
296	30	0.94	0.9	-3.2	+83	-0.143	-0.09	+0.003
296	110	0.95	1.1	-3.2	+81	-0.097	-0.07	+0.003
323	110	0.95	1.2	-3.5	+81	-0.066	-0.06	+0.003

and $\rho(\Omega, \mathbf{R})$ is the single particle density function, which satisfies the normalization condition $\int d\mathbf{R}d\Omega\rho(\mathbf{R}, \Omega) = N$. The interaction between virions is described by the function

$$u(\mathbf{R}_{AB}, \Omega_{AB}) = -k_B T e_{AB}^h(\mathbf{R}_{AB}, \Omega_{AB}) + g_h(\mathbf{R}_{AB}, \Omega_{AB}) U^{\text{el}}(\mathbf{R}_{AB}, \Omega_{AB}), \quad (2)$$

where e_{AB}^h is the Mayer function for a pair of hard particles [19], g_h is the hard-particle pair distribution function, and $U^{\text{el}}(\mathbf{R}_{AB}, \Omega_{AB})$ is the electrostatic potential between a pair of polyelectrolytes. The density function $\rho(\Omega, \mathbf{R})$ can be written in terms of the orientation of the local director in \mathbf{R} , thus of the twist wave number q , and of orientational order parameters with respect to the director, \overline{P}_J (even J). It follows that the free energy can in turn be expressed as a function of twist deformation and orientational order parameters. In view of their large length scale, twist deformations can be assumed to negligibly disturb the local order; \overline{P}_J values can then be obtained by minimizing the free energy of the undeformed nematic phase. Finally, chiral strength and twist elastic constant are evaluated as derivatives of the free energy density with respect to the twist deformation.

A coarse-grained representation of the virus structure has been used to parametrize interactions. Starting from atomic coordinates [8], the model shown in Fig. 1(c) has been built. Three negative point charges have been placed on each protein. Two of them, located on outer spheres, roughly correspond to protruding ionic amino acids, while the third, placed within the groove, accounts for the excess of electron density on solvent exposed oxygen atoms in the protein backbone. For simplicity, the three charges have been assumed to be equivalent. The electrostatic interaction between a pair of virus particles can be approximated as the superposition of screened Coulomb interactions between their (renormalized) charges [20]. However, this is not appropriate for charges at short distance and solvent confined between close surfaces. At the contact distance between the spheres bearing a pair of interacting charges, the electrostatic potential seems better expressed by the Coulomb law in a nonpolar medium. To keep calculations feasible, a simple choice has been made: the electrostatic potential between two charges is assumed to have the Coulomb form at the contact separation and the screened Coulomb form beyond a reference distance, r_0 ; for inter-

mediate distances, an interpolation between the boundary values is performed [16]. In view of the dimension of the grooves, r_0 has been given the value of 1 nm. The integrals over mutual orientations and distances of a pair of virions, necessary for obtaining the free energy and its derivatives, are calculated numerically. The full virion is considered and, given the form of the Mayer function, the excluded volume contribution only needs to be evaluated over overlapping configurations. In the electrostatic part, the pair distribution function is simply chosen equal to the step function: $g_h = 0$ or $g_h = 1$, for overlapping and nonoverlapping pair configurations, respectively; thus, electrostatic integrals are evaluated over nonoverlapping pair configurations. Computing time is significantly reduced by exploiting symmetries and introducing cutoff distances for the screened electrostatic interactions. Moreover, a simplified virus model has been adopted to calculate order parameters and twist elastic constant, which are scarcely affected by the short length scale features of the system: a virus has been represented as a rod of fused spheres, while keeping the charge distribution shown in Fig. 1(c).

Experimental and theoretical results are collected in Table I. Electrostatic interactions have a small effect on order parameters and twist elastic constant, which substantially are of steric nature. High \overline{P}_2 values are obtained, slightly larger than those determined for M13 under analogous conditions by birefringence measurements [21]. Experimental K_{22} data are available for *fd* virus; $K_{22} \sim 0.4$ pN has been reported from measurements of the critical magnetic field [10], which is about half the predicted value. Electrostatic (K_t^{el}) and steric (K_t^h) contributions to the chiral strength have *opposite* sign; the latter yields a right-handed supramolecular helix which, in agreement with Straley's model [14], provides the best packing of a system of hard right-handed helices like those outlined in Fig. 1. Electrostatic interactions give an antagonist contribution to the chiral strength, which can be interpreted as the result of the repulsions arising when helices fit into each other's grooves. Indeed, electrostatic repulsions are maximized in those configurations which are favored for steric reasons, because charges of equal sign lie at close distance. The electrostatic term largely overcomes the steric one; therefore, a left-handed cholesteric phase is predicted, as experimentally observed. The electrostatic contributions to the free energy and to its derivatives scale as Q^2 , the square of point charges. The values reported in

Table I have been obtained with $Q = -0.3e$, i.e., one fourth of the bare charges. This corresponds to a degree of charge compensation which is a little lower than predictions of the Manning theory [22]; however, the model of a uniform line charge distribution can only yield very approximate estimates for the system under investigation. The cholesteric wave number, $q = -(K_t^{\text{el}} + K_t^h)/K_{22}$, is also reported in Table I. In agreement with experiment, the cholesteric pitch is predicted to increase with increasing temperature and ionic strength. In the case of a purely entropic mechanism the pitch would be independent not only of ionic strength, but also of temperature, since elastic constant and chiral strength would have the same linear dependence of T .

In summary, we have experimentally investigated the cholesteric phase of M13 virus and we have shown that the main findings can be explained by a model accounting for steric and electrostatic interactions between rigid chiral rods. The model relies on a realistic representation, although at a coarse-grain level, of what are deemed to be the relevant molecular features for chirality amplification: the shape chirality deriving from the arrangement of the coat proteins, and the associated helical distribution of charges. The predicted pitch and handedness depend on the structure of the coat proteins, and are expected to change with it. It must be mentioned that in the model presented here some simplifying assumptions have been taken. Beside the simple treatment of electrostatics, a major approximation is the neglect of virus flexibility, which is expected to affect order and elastic properties of the system and to introduce its own dependence on temperature and ionic strength. Moreover, changes in the physicochemical conditions are likely to bring about modifications in structure and arrangement of coat proteins, which are not accounted for by our model. This work singles out a general feature in the phenomenon of chirality amplification, i.e., *the simultaneous presence of oppositely handed contributions at the molecular scale* [6,23]. Only in the particular and rather unrealistic case of hard-core interactions between screwlike molecules, a simple link from molecular to phase helicity exists [14].

E. G. warmly thanks G. Gourges and P. Sirand-Pugnet from I.N.R.A. for their assistance in the preparation of the viruses. F.T. and A.F. acknowledge financial support by MIUR (No. PRIN 2005).

- [1] Z. Dogic and S. Fraden, in *Soft Matter*, edited by G. Gompper and M. Schick (Wiley-VCH, Weinheim, 2006), Vol. 2.
- [2] J. Lapointe and D. A. Marvin, *Mol. Cryst. Liq. Cryst.* **19**, 269 (1973).
- [3] L. Onsager, *Ann. N.Y. Acad. Sci.* **51**, 627 (1949).
- [4] A. Stroobants *et al.*, *Macromolecules* **19**, 2232 (1986).
- [5] A. P. Lyubartsev *et al.*, *Phys. Rev. Lett.* **81**, 5465 (1998).
- [6] A. B. Harris *et al.*, *Rev. Mod. Phys.* **71**, 1745 (1999).
- [7] E. Grelet and S. Fraden, *Phys. Rev. Lett.* **90**, 198302 (2003).
- [8] D. A. Marvin *et al.*, *J. Mol. Biol.* **355**, 294 (2006). M13 differs from *fd* for replacement of a negatively charged Aspartate with a neutral Asparagine in the coat protein.
- [9] D. S. Thiriot *et al.*, *J. Mol. Biol.* **341**, 869 (2004).
- [10] Z. Dogic and S. Fraden, *Langmuir* **16**, 7820 (2000).
- [11] S. Bhattacharjee *et al.*, *Biophys. J.* **61**, 725 (1992); A. C. Zeri *et al.*, *Proc. Natl. Acad. Sci. U.S.A.* **100**, 6458 (2003); L. C. Welsh *et al.*, *Macromolecules* **29**, 7075 (1996).
- [12] K. Zimmermann *et al.*, *J. Biol. Chem.* **261**, 1653 (1986).
- [13] M13 was grown using the XL1-Blue strain of *E. Coli* as the host bacteria and purified following standard biological protocols [1]. To vary the ionic strength, viruses have been dialyzed against a 20 mM TRIS-HCl buffer at pH = 8.2 with an adjusted amount of NaCl. Virus concentrations have been measured by spectrophotometry. For fluorescence microscopy experiments, M13 has been labeled with fluorescein isothiocyanate (FITC).
- [14] J. P. Straley, *Phys. Rev. A* **14**, 1835 (1976).
- [15] D. H. Van Winkle *et al.*, *Macromolecules* **23**, 4140 (1990); F. Livolant and A. Leforestier, *Prog. Polym. Sci.* **21**, 1115 (1996).
- [16] F. Tombolato and A. Ferrarini, *J. Chem. Phys.* **122**, 054908 (2005).
- [17] G. Kishchenko *et al.*, *J. Mol. Biol.* **241**, 208 (1994).
- [18] P. G. de Gennes and J. Prost, *The Physics of Liquid Crystals* (Clarendon, Oxford, 1993).
- [19] J. P. Hansen and I. R. McDonald, *Theory of Simple Liquids* (Academic, New York, 1986).
- [20] J.-P. Hansen and H. Löwen, *Ann. Rev. Phys. Chem.* **51**, 209 (2000).
- [21] K. R. Purdy and S. Fraden, *Phys. Rev. E* **70**, 061703 (2004).
- [22] G. Manning, *J. Chem. Phys.* **51**, 924 (1969).
- [23] R. L. B. Selinger *et al.*, *Phys. Rev. Lett.* **93**, 158103 (2004).
- [24] Surface generated using DS ViewerPro 5.0 software.